



Earthquake Analysis Suggests Dyke Intrusion in 2019 Near Tarawera Volcano, New Zealand

Thomas W. Benson¹, Finnigan Illsley-Kemp^{1*}, Hannah C. Elms¹, Ian J. Hamling², Martha K. Savage¹, Colin J. N. Wilson¹, Eleanor R. H. Mestel¹ and Simon J. Barker¹

¹School of Geography, Environment and Earth Sciences, Victoria University of Wellington, Wellington, New Zealand, ²GNS Science, Avalon, New Zealand

OPEN ACCESS

Edited by:

Francesco Maccaferri,
Vesuvius Observatory, National
Institute of Geophysics and
Volcanology (INGV), Italy

Reviewed by:

Yohei Yukutake,
Hot Spring Geology Research
Institute, Japan
Francesca Di Luccio,
Istituto Nazionale di Geofisica e
Vulcanologia (INGV), Italy

*Correspondence:

Finnigan Illsley-Kemp
finnigan.illsleykemp@vuw.ac.nz

Specialty section:

This article was submitted to
Solid Earth Geophysics,
a section of the journal
Frontiers in Earth Science

Received: 16 September 2020

Accepted: 11 November 2020

Published: 14 January 2021

Citation:

Benson TW, Illsley-Kemp F, Elms HC,
Hamling IJ, Savage MK, Wilson CJ N,
Mestel ERH and Barker SJ (2021)
Earthquake Analysis Suggests Dyke
Intrusion in 2019 Near Tarawera
Volcano, New Zealand.
Front. Earth Sci. 8:606992.
doi: 10.3389/feart.2020.606992

Tarawera volcano (New Zealand) is volumetrically dominated by rhyolitic lavas and pyroclastic deposits, but the most recent event in AD 1886 was a basaltic Plinian fissure eruption. In March 2019 a swarm of at least 64 earthquakes occurred to the NE of Tarawera volcano, as recorded by the New Zealand Geohazard Monitoring Network (GeoNet). We use seismological analysis to show that this swarm was most likely caused by a dyke that intruded into the brittle crust between depths of 8–10 km and propagated toward Tarawera volcano for 2 km at a rate of 0.3–0.6 m s⁻¹. We infer that this was a dyke of basaltic composition that was stress-guided toward Tarawera volcano by the topographic load of the volcanic edifice. Dyke intrusions of this nature are most likely a common occurrence but a similar process may have occurred during the 1886 eruption with a dyke sourced from some lateral distance away from the volcano. The 2019 intrusion was not detected by InSAR geodesy and we use synthetic models to show that geodetic monitoring could only detect a ≥6 m wide dyke at these depths. Improvements to geodetic monitoring, combined with detailed seismological analysis, could better detect future magmatic intrusions in the region and serve to help assess ongoing changes in the magmatic system and the associated possibilities of a volcanic event.

Keywords: dyke intrusion, volcano seismicity, seismology, volcanology, InSAR, Okataina Volcanic Center, Tarawera volcano

1. INTRODUCTION

Forecasting volcanic eruptions is inherently challenging due to the wide range of unrest signals (e.g., ground deformation, elevated seismicity, gas emissions) that can occur at variable rates and over variable timescales prior to eruption (e.g., Sparks et al., 2012). Many of these unrest signals can also occur without leading to eruption, highlighting the complex nature of the subsurface plumbing systems and the numerous processes that occur beneath dormant volcanoes (Moran et al., 2011). Monitoring subsurface processes is important for developing an understanding of how different volcanoes operate and for assessing any deviation from the normal background state (e.g., Cashman and Sparks, 2013; Acocella, 2014).

Many of the challenges with assessing volcanic unrest are exemplified with caldera volcanoes, which are among the most complex and dangerous types of volcano (Acocella et al., 2015). Caldera volcanoes often cover a wide geographical area (up to several ten of kilometers wide) with large, geometrically complex and heterogeneous magmatic systems that are capable of producing explosive eruptions, sometimes of great size. However, understanding of the current state of these systems is

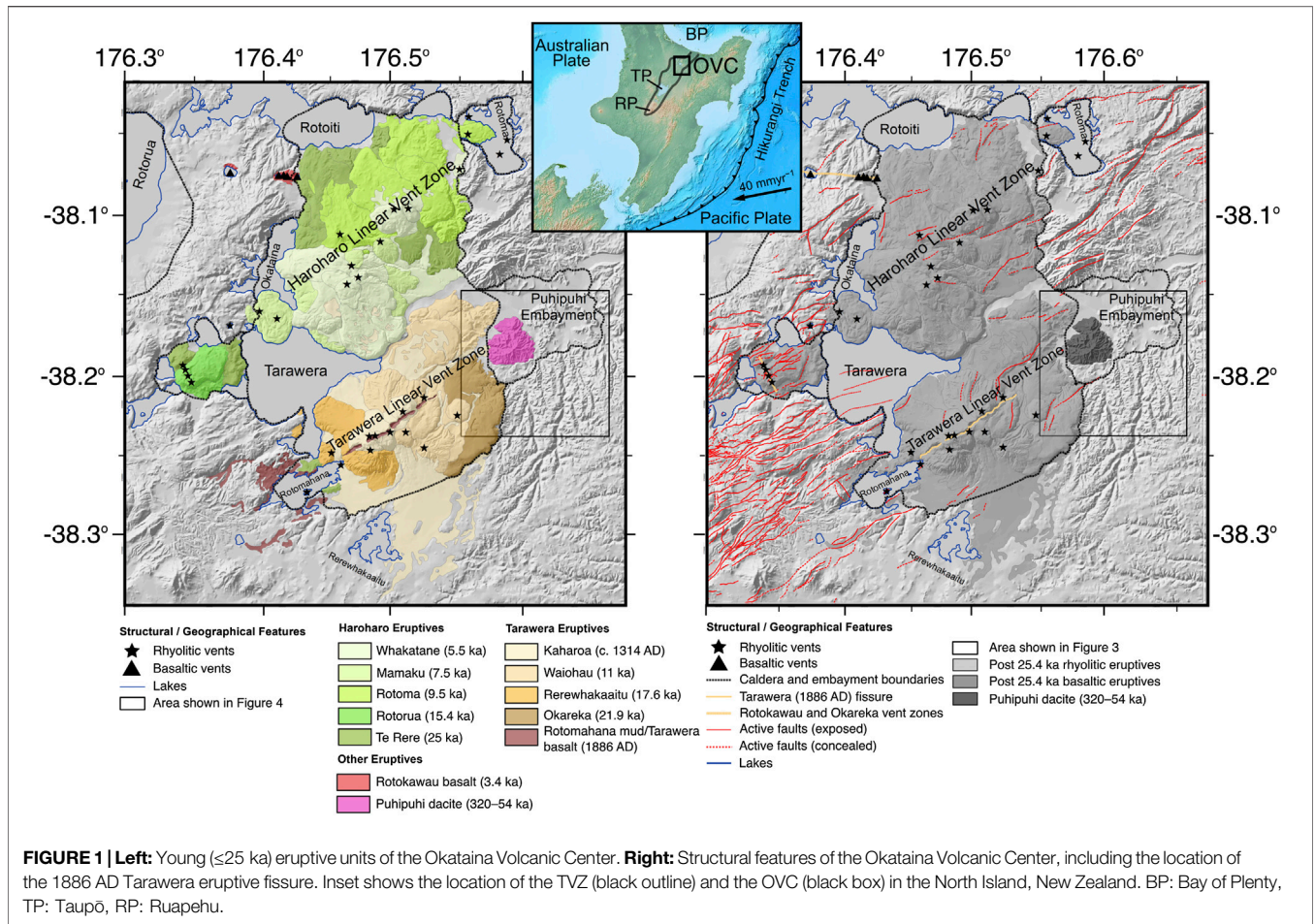


FIGURE 1 | Left: Young (≤ 25 ka) eruptive units of the Okataina Volcanic Center. **Right:** Structural features of the Okataina Volcanic Center, including the location of the 1886 AD Tarawera eruptive fissure. Inset shows the location of the TVZ (black outline) and the OVC (black box) in the North Island, New Zealand. BP: Bay of Plenty, TP: Taupō, RP: Ruapehu.

often made complex by the presence of active, shallower hydrothermal systems and fault structures (e.g., Sandri et al., 2017; Mantiloni et al., 2020). Disentangling the signals of magmatic unrest (e.g., variations in the pressure of the system due to magma recharge or ascent) vs. non-magmatic unrest (e.g., changes in the hydrothermal system or tectonic earthquakes) can be difficult, with the potential for many different mechanisms that can produce similar unrest symptoms (Acocella et al., 2015).

Here we document and interpret a series of earthquakes that occurred over a 3 day period near Tarawera volcano (New Zealand) in March 2019. Tarawera is the site of a large basaltic fissure eruption in AD 1886, but is positioned within a larger caldera structure that has a history of producing high-silica (rhyolitic) magmas (Figure 1). As such, it is important to constrain the origin of these earthquakes and to consider how they relate to the modern magmatic system and ongoing activity in the broader region around the caldera.

2. GEOLOGICAL BACKGROUND

The Taupō Volcanic Zone (TVZ) in the central North Island of New Zealand (Figure 1) has been volcanically active since approximately 2 Ma, and from 1.85 Ma eruptions have been

dominated by high-silica (rhyolitic) magmas (Eastwood et al., 2013; Chambefort et al., 2014). The TVZ can be subdivided into three segments along its length. The southern and northern segments are characterized by andesite volcanism building composite cones, whereas the central TVZ is dominated by voluminous rhyolite volcanism associated with caldera volcanoes and unusually high surface heat-flow (Bibby et al., 1995; Wilson et al., 1995). Over the last 50–60 kyr this rhyolitic volcanism has mainly been focused at Taupō and Okataina volcanoes, at the southern and northern limits of the central TVZ respectively. The TVZ also hosts the Taupō continental rift with present-day rates of extension increasing from ≤ 5 mm/yr at Ruapehu in the south, to 13–19 mm/yr at the Bay of Plenty coastline and increasing farther offshore (Wallace et al., 2004; Lamarche et al., 2006). The orientation of present-day extension within the Taupō rift varies from rift-orthogonal in the south to oblique in the north (Rowland and Sibson, 2001; Acocella et al., 2003; Townend et al., 2012; Seebeck et al., 2014; Illsley-Kemp et al., 2019). Several studies have suggested that extension within the Taupō rift is partially accommodated by magmatic intrusions (Rowland et al., 2010), however this may not be ubiquitous throughout the rift (Villamor et al., 2011).

The Okataina Volcanic Center (OVC) is built on a system of nested calderas formed by multiple large-volume rhyolite

eruptions over at least the last ~340 kyr (Nairn, 2002; Cole et al., 2010, 2014) (**Figure 1**). Over the past ~25 kyr volcanism has been focused at the Haroharo and Tarawera volcanic complexes, in the northern and southern parts of the OVC, respectively (Nairn, 2002). Both complexes are volumetrically dominated by rhyolitic eruptive products, including voluminous lavas forming the respective edifices, erupted from vents aligned along two linear vent zones. A notable feature is that rhyolitic eruptions from the Tarawera complex have often been associated with basaltic intrusion and eruption. The most recent rhyolite eruption (the AD 1314 ± 10 Kaharoa eruption from the Tarawera complex; Hogg et al., 2003) was primed and triggered by the intrusion of primitive basalt (containing primitive olivines; Barker et al., 2020) that was mixed into the rhyolite magma reservoir (Leonard et al., 2002; Nairn et al., 2004). There is also evidence that many of the previous rhyolite eruptions from the Tarawera complex had basaltic input/interaction (Nairn, 1992; Darragh et al., 2006; Shane et al., 2007; Shane et al., 2008). The composition of basaltic magmas erupted from the OVC show little variation between eruptions but they are distinct in their composition compared to basalts erupted outside the caldera to the south (Barker et al., 2020).

The influence of basaltic magmatism at the OVC was most dramatically illustrated in the AD 1886 Tarawera basaltic Plinian eruption, sourced from a ~17 km long fissure (Nairn, 1979; Walker et al., 1984; Sable et al., 2006) (**Figure 1**). However, the 1886 eruptive products show no physical evidence for any interaction with a melt-dominant rhyolite magma reservoir, only shallow xenolithic incorporation (Cole, 1970; Cole et al., 2014; Carey et al., 2007; Carey and Houghton, 2010), although some crustal contamination is indicated from trace element and isotopic data (Gamble et al., 1993; Waight et al., 2017). The inference, therefore, is that the feeder dyke rose from the base of the quartzofeldspathic crust and ascended rapidly while avoiding any interaction with evolved melt-rich magmatic reservoirs. The location of this primitive source, and the pathway of the eruptive dyke are largely unknown. Nairn and Cole (1981) document the 1886 eruptive fissures and find that the surface dykes are arrayed in a left-stepping en-echelon pattern within a larger fissure structure. The dykes have a common orientation of ~70°, while the eruptive fissure strikes at ~60°. This led Nairn and Cole (1981) to suggest that orientation of the dyke intrusions reflect the modern day orientation of maximum horizontal compression (SH_{max}), whereas the eruptive fissure reflects the orientation of an older fault structure. Vents during the eruption began at two locations at the Tarawera summit and spread both NE (for a short distance) and SW (for ~11 km) along the fissure line during the course of the eruption (Sable et al., 2006).

In addition to the ample evidence that dyke intrusions, specifically of basaltic composition, play an important role in OVC eruptions, they are also thought to play a key role in the accommodation of extension in the Taupō rift (Rowland et al., 2010; Villamor et al., 2011). However, while dyke-accommodated rifting has been directly observed in other continental rifts (Kendall et al., 2005; Ebinger et al., 2013) and realistically has

to have occurred during the 1886 eruption, it has not yet been detected in the TVZ in the modern instrumental era. Analysis of GPS data from the OVC area found that strain in the region surrounding the Tarawera fissure should promote the intrusion of dykes (Holden et al., 2015). Other geodetic studies, however, found that the OVC and TVZ are more accurately described as contractional areas at present (Hamling et al., 2015; Dimitrova et al., 2016; Haines and Wallace, 2020).

Knowledge of the modern-day location or state of the magmatic system(s) at OVC is limited. Electrical resistivity imaging shows evidence for a broadly distributed low-resistivity structure across the OVC between 10 and 20 km depth (Heise et al., 2010) and a region of partial melt to the SW of the OVC at depths ≥8 km (Heise et al., 2016). In contrast, seismic anisotropy suggests the presence of a large upper-crustal magma body (Illsley-Kemp et al., 2019). Earthquake activity in the OVC is highly swarm-like, and in the instrumental era (post-1985) has been largely limited to the Haroharo complex and to the southwest of Tarawera beneath Lake Rotomahana, outside the OVC caldera (Hurst et al., 2008; Bannister et al., 2016) (**Figure 1**). The Lake Rotomahana earthquake activity is thought to be caused by geothermal fluid migration along sub-surface faults between 4 and 7 km depth (Bannister et al., 2016). Eruptive histories and phenocryst mineralogies for the ≤25 ka products of the OVC suggest that Haroharo and Tarawera have different upper crustal magmatic systems, albeit at comparable depths (Cole et al., 2014). Petrological studies based on volatile concentrations in quartz-hosted melt inclusions have suggested storage pressures for the erupted rhyolitic magmas in the range of 130–160 MPa (5–7 km) for most examples (Johnson et al., 2011) with greater depths (to ~12 km) proposed for some (Shane et al., 2007). Also, the presence of cummingtonite as a phenocryst phase in many of the young Okataina rhyolites indicates similar maximum pressures and depths (Nicholls et al., 1992). An improved understanding of the modern system would assist with the monitoring of the volcanoes, particularly as studies by Sherburn and Nairn (2004) and Holden et al. (2017) suggest that it may be possible for significant subsurface magmatic activity to occur in the OVC without detection by the geodetic monitoring currently in place. Building a better understanding of modern magmatic activity is also important for constraining tipping points that could result in magmatic activity/unrest at the OVC cascading toward major unrest and/or eruption (Acocella et al., 2015; Wilson, 2017). In this regard, it is significant that on March 12, 2019, the New Zealand Geohazard Monitoring Network (GeoNet) recorded a cluster of 64 earthquakes to the northeast of Tarawera volcano. In this paper we investigate this seismic cluster and its cause in more detail.

3. DATA AND METHODS

For this study, we downloaded continuous seismic data from March 12, 2019 to March 15, 2019 (inclusive) from seven short-period GeoNet seismometers (**Figure 2**). We manually detected earthquakes within the continuous data and picked all visible P

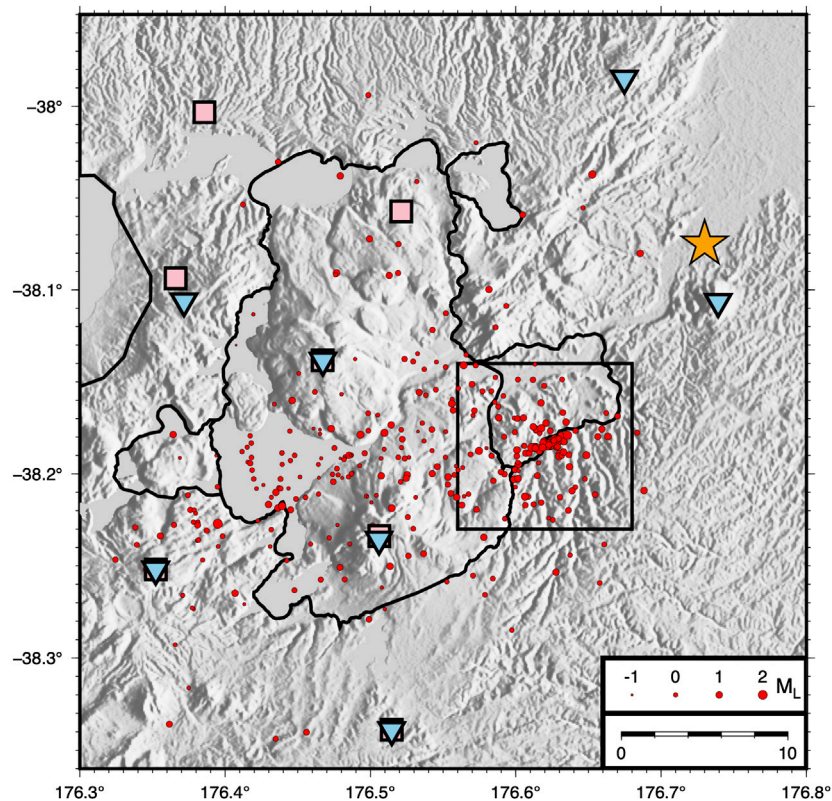
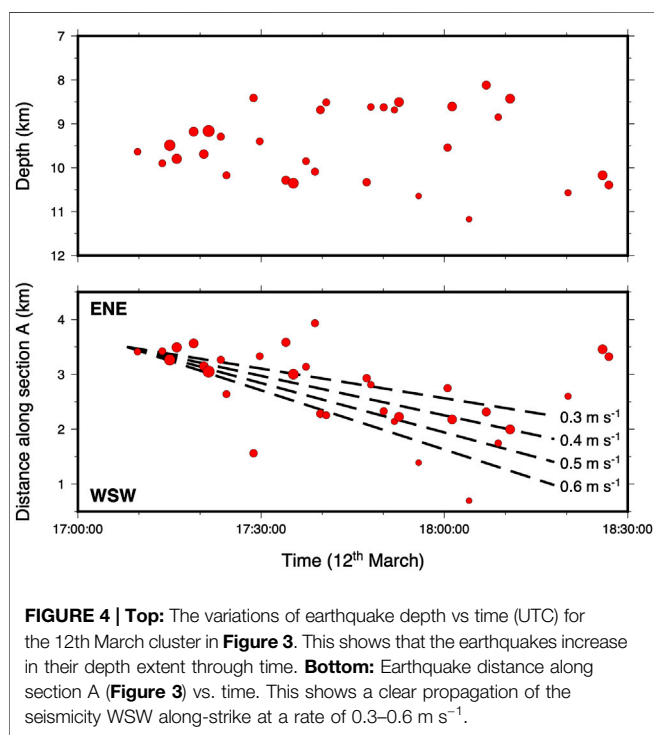
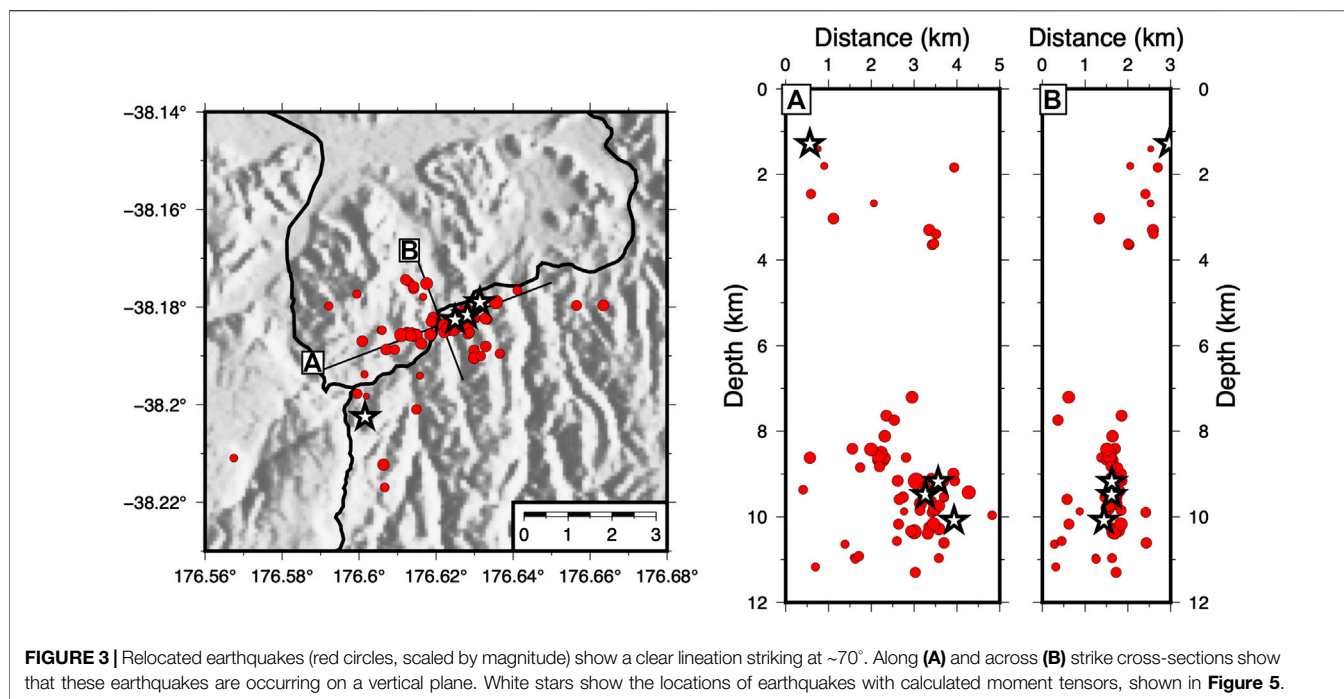


FIGURE 2 | Map of 348 earthquakes (red circles, scaled by magnitude) that occurred in the Okataina region between the 12th–15th March 2019. The blue inverted triangles denote the seven short-period GeoNet seismometers used to detect and locate the earthquakes. Pink squares denote the location of the GeoNet GNSS network. The black box shows the location of **Figure 3**. The orange star marks the location of Kawerau geothermal field, where the velocity model used in this study was derived (Clarke et al., 2009, Figure S1).

and S phase-arrivals resulting in a total of 348 earthquakes. These earthquakes were initially located with NonLinLoc (Lomax et al., 2000), using a velocity model derived from the nearby Kawerau geothermal field (Clarke et al., 2009) (**Supplementary Figure S1**). We then used waveform correlation to generate differential pick times with the Obspy package (Beyreuther et al., 2010). We used a 2 s window around each pick, beginning 0.5 s before the pick, allowing the pick to adjust by up to 0.3 s, and each event pair had a maximum hypocentral separation of 8 km. These differential pick times were then used to relocate the entire catalog using the double-difference relocation program GrowClust (Trugman and Shearer, 2017), requiring a minimum correlation of 0.5. This resulted in 94 relocated earthquakes in total (**Figure 2**). We calculate local-magnitudes by measuring the peak displacement on a simulated Wood-Anderson seismometer on each seismometer, for each earthquake. We then use the local-magnitude scale developed for New Zealand (Ristau et al., 2016). This results in magnitudes over the range -1.12 to $2.54 M_L$, and for earthquakes also detected by GeoNet our magnitudes are comparable. We then compute moment tensors using P-wave polarities picked on the wider North Island GeoNet network and the Bayesian moment tensor source inversion software MTfit (Pugh and White, 2018).

4. RESULTS

The main concentration of earthquakes (131 events total, 71 relocated) occurred in the Puhipuhi embayment to the northeast of Tarawera (**Figure 3**) and ranged from -0.47 to $2.54 M_L$ in magnitude. The mean horizontal and vertical errors from the initial location are ± 0.8 and ± 0.68 km respectively, and the relative horizontal and vertical errors after relocation are ± 0.036 and ± 0.005 km, respectively. The relocated earthquakes form a clear lineation with a strike of $\sim 70^\circ$. When viewed in cross-section the earthquakes appear to have occurred along a ~ 3 km long, vertical plane between 8 and 10.5 km depth (**Figure 3**). The earthquakes migrated from NE to SW at an apparent rate of 0.3 – 0.6 m s^{-1} , and their range of depths increased at the same time (**Figure 4**). These spatial patterns are also produced when using locations generated using GrowClust's internal bootstrapping approach (Efron and Tibshirani, 1991; Efron and Tibshirani, 1994; Trugman and Shearer, 2017), demonstrating that they are not an artifact of data or station distribution (**Supplementary Figures S1, S2**). We are able to calculate four reliable moment tensor solutions for earthquakes in this swarm (**Figure 5**). These all produce double-couple, normal fault solutions with nodal plane strikes very similar to the strike of the earthquake cluster lineation. The

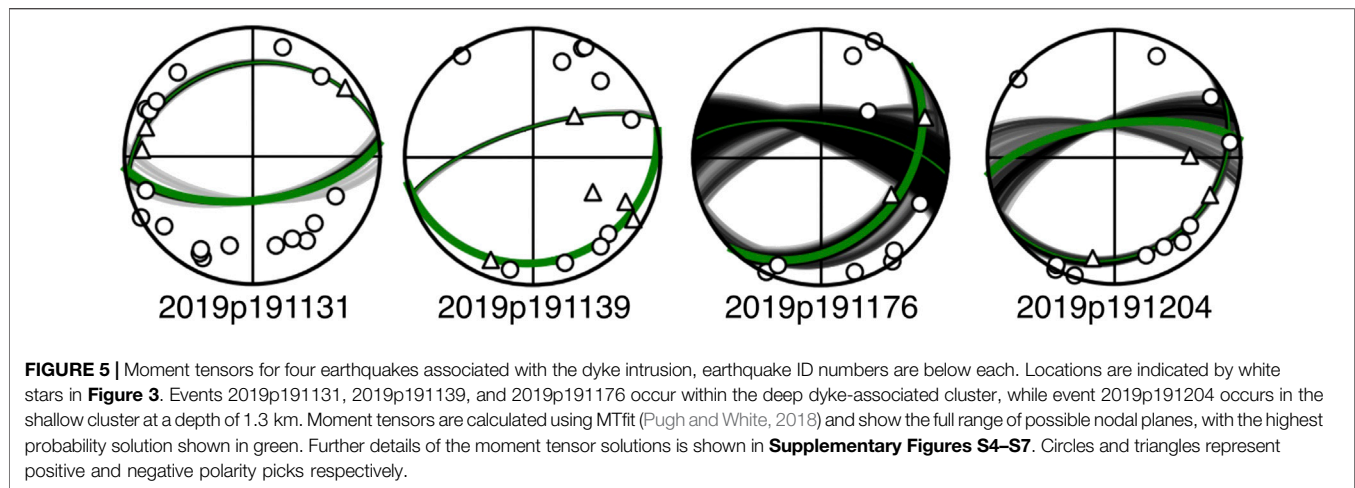


three solved moment-tensors which occur within the dyke-cluster (2019p191131, 2019p191139, 2019p191176) can be solved with a non-double-couple component but as a double-couple solution can adequately explain the data, we select this as the least complicated solution (**Supplementary Figures S4–S7**).

5. DISCUSSION

5.1. Origin of the 2019 Earthquake Swarm

The March 2019 earthquake cluster has several notable characteristics. First, it delineates a vertical structure between ~ 8 and 10.5 km depth (**Figure 3**), which is close to the base of the generally observed seismogenic depth in the TVZ (Bryan et al., 1999). Second, the vertical structure has a strike of $\sim 70^\circ$ (**Figure 3**), near identical to the observed surficial orientation of dyke intrusions during the 1886 Tarawera eruption (Nairn and Cole, 1981). Third, the earthquakes migrated laterally, from ENE to WSW, at a rate of $0.3\text{--}0.6\text{ m s}^{-1}$ and their depth distribution range expanded during this lateral migration (**Figure 4**). There are three possible causes for earthquake swarms in the TVZ; slip on a fault-plane, diffusion of geothermal fluids, or intrusion of a magmatic body. Given that the earthquake cluster occurs below the brittle-ductile transition in the TVZ (Bryan et al., 1999) and occurs along a vertical plane, inconsistent with extensional faulting, we suggest it is unlikely that the cluster was caused by slip along a fault-plane. Lateral propagation of seismicity along vertically inclined faults has been observed at oceanic transform faults and interpreted as aseismic creep along a fault-plane (Roland and McGuire, 2009). While these observations are similar to those presented here, the tectonic setting in the TVZ is quite different and we feel it is therefore unlikely that our observations are explained by strike-slip creep. Smith et al. (2007) proposed that subsidence at Taupō caldera (New Zealand) in 1983 was caused by the dewatering of a magma body at depth, and at Yellowstone caldera (USA) this process has been shown to cause propagating seismicity on a vertical plane, similar to our observations (Waite and Smith, 2002). However, the diffusion velocity of hydrothermal fluids resulting from dewatering is



estimated, and observed, to be several orders of magnitude slower than the intrusion rate we observe, and thus our data is not satisfactorily explained by the diffusion of geothermal fluids from a dewatering magma body. In addition, upwelling geothermal fluids have been observed to cause seismicity in nearby Rotomahana (Bannister et al. 2016; **Figure 1**). However, the seismicity at Rotomahana shows no lateral migration, occurs between 4 and 6.5 km depth, and occurs in repetitive “bursts” over at least the past 25 years (Bannister et al., 2016). These characteristics suggest that the March 2019 earthquake cluster is unlikely to be caused by a similar upwelling of geothermal fluids.

We therefore suggest that the 2019 earthquake swarm was most likely caused by a dyke, intruding to depths as shallow as ~8–10.5 km, that migrated toward Tarawera volcano in a WSW direction. The migrating earthquakes are inferred to have been caused by country rock opening at the tip of the propagating dyke (Belachew et al., 2011; Sigmundsson et al., 2015), and this is evidenced by the normal fault moment tensors (**Figure 5**). These moment tensors may also be explained by a component of non-double-couple deformation (**Supplementary Figures S4–S7**), which would also support a dyke model. We can thus use the migration rate of earthquakes as a proxy for the intrusion rate of the dyke (i.e. $0.3\text{--}0.6\text{ m s}^{-1}$). Our calculated intrusion rate of $0.3\text{--}0.6\text{ m s}^{-1}$ is very similar to those recorded for basaltic dyke intrusions in the Afar rift (Belachew et al., 2011; Barnie et al., 2015), Red Sea (Eyles et al., 2018), El Hierro (Martí et al., 2013), and Iceland (Einarsson and Brandsdóttir, 1980). However, it is significantly faster than intrusion rates calculated from a rhyolite dyke intrusion in the Main Ethiopian Rift ($3 \times 10^{-3}\text{ m s}^{-1}$; Temtime et al., 2020). We therefore propose that the dyke intrusion was most likely basaltic in composition.

5.2. Volume Estimate

Dyke intrusions represent movement of magma that can often be detected by volcanic monitoring through measuring surface deformation. However, the ability to detect intrusions depends on many factors including the volume and location of the intrusion. Based on the energy balance caused by an intrusion

and the seismic moment release, Bonaccorso et al. (2017) derived an empirical relationship relating seismic moment to dyke thickness. Using this relationship, and the total seismic moment release of $1.77 \times 10^{13}\text{ N m}$, the thickness of the 2019 dyke near Tarawera would be ~0.15 cm. Alternatively, global observations of dyke intrusions suggest length to thickness ratios of 1,500 (Gudmundsson, 1987, 2011) giving a thickness of ~2 m. Therefore, based on the dyke’s length and associated seismic moment release, we could expect an intrusion with a volume of $1.1\text{--}15 \times 10^6\text{ m}^3$. Ground deformation as a result of discrete dyking events has been well documented in a number of volcanic and rift environments (Hamling et al., 2009; Sigmundsson et al., 2015; Hamling et al., 2019). To investigate whether the inferred dyke was detected geodetically, we use ascending and descending synthetic aperture radar (SAR) data acquired by the Sentinel-1 satellite to generate two co-intrusion interferograms (**Figure 6**). Neither of the interferograms show an obvious signal consistent with an intrusion, and there is no detectable signal in the GNSS network (**Figure 2**). However, given the depth of the dyke intrusion, it is possible that ground deformation was too small to be detected.

To investigate how much volume could be hidden before deformation would be detected by the InSAR data, we generated a suite of synthetic intrusions. We fixed the geometry of the dyke based on the earthquake observations and examined the effect of the dyke thickness on the detectable signal. For each thickness value, we generated a synthetic interferogram by adding the modeled deformation to the ascending and descending interferograms respectively. We then evaluated the signal to noise ratio using the deformation from the modeled intrusion as the reference signal. For both the ascending and descending datasets, the signal to noise ratio only becomes positive once the thickness of the dyke exceeds ~5–6 m (**Figure 6**). This suggests that for a similar sized intrusion, at these depths, we would be unlikely to detect it with current geodetic monitoring unless its volume exceeds $\sim 37\text{--}45 \times 10^6\text{ m}^3$.

Our estimated intrusion volume of $1.1\text{--}15 \times 10^6\text{ m}^3$, based on dyke length and seismic moment release, should be considered as a minimum estimate, as the maximum depth of the

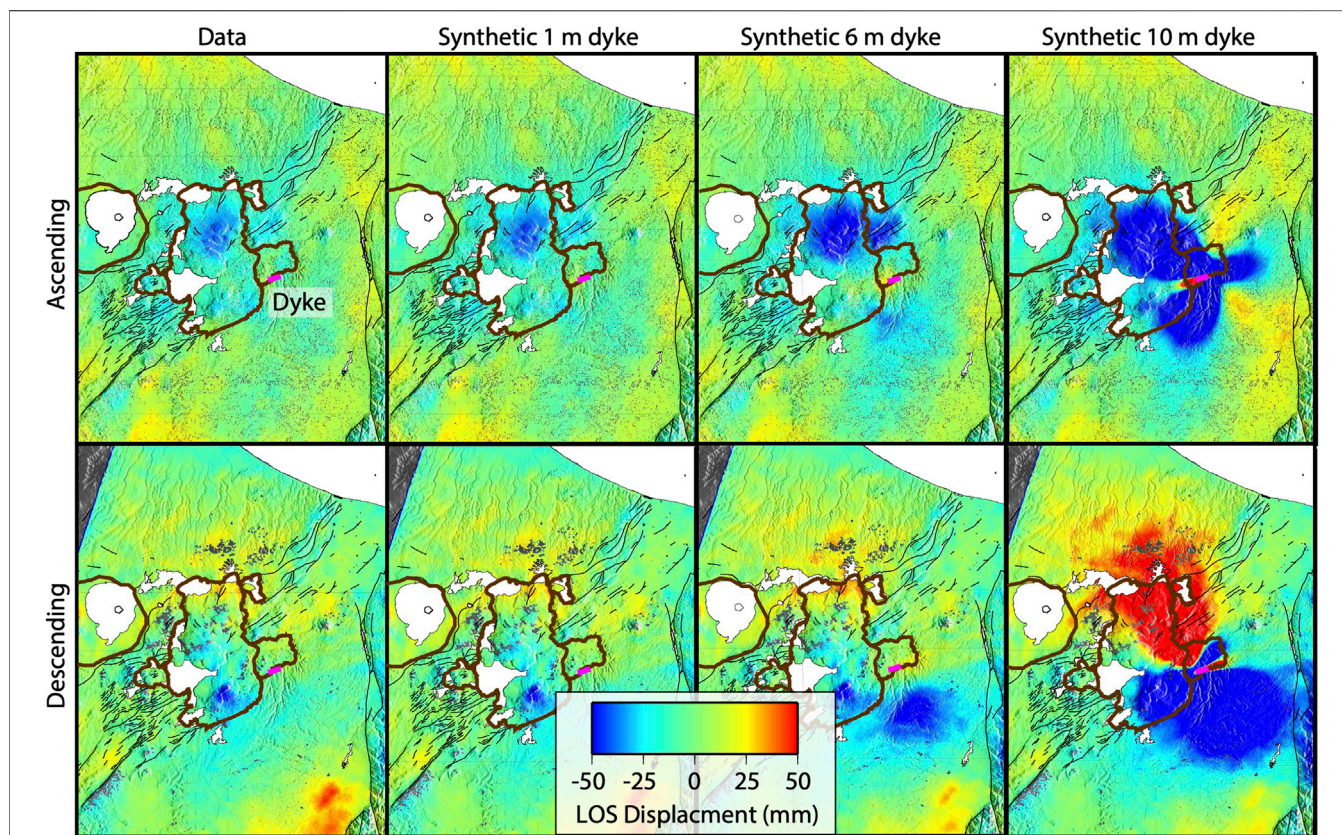


FIGURE 6 | Line of site displacement for ascending (**top**) and descending (**bottom**) SAR data acquired by Sentinel-1. The data (**left**) shows no observable ground deformation from the dyke intrusion. We then use synthetic dykes, centered on the 2019 dyke location but with varying thickness, to show that only a dyke intrusion with thickness ≥ 6 m would be detectable.

earthquake sequence may not provide a lower limit on the intrusion. Evidence from elsewhere in the TVZ (e.g., Bryan et al., 1999), suggests the depths of the earthquake sequence may only reflect the maximum depth to which brittle failure occurred. It is therefore likely that the source reservoir for the 2019 dyke intrusion lies at depths ≥ 10 km in the vicinity of the Puhipuhi embayment. Further geophysical imaging in this region may be able to determine the location and depth of this magma reservoir.

5.3. Structural and Magmatic Implications

Our results lend contemporary evidence to the suggestion of Villamor et al. (2011) that extension within the OVC is accommodated by dyke intrusions. We also observe shallow (1–4 km depth) earthquakes directly above the dyke during intrusion (Figure 3), this is most likely caused by dyke-induced mechanical faulting accommodating extension in the brittle shallow crust (e.g., Belachew et al., 2011). Dyke intrusions can also yield good indications of the orientation of the crustal stress field (Wadge et al., 2016). The orientation ($\sim 70^\circ$) of this dyke intrusion suggests that this is also the orientation of the maximum horizontal compression (SH_{max}). This orientation differs slightly to observations from the rest of the TVZ which suggest an SH_{max} orientation of 40° – 60° (Townend et al., 2012; Illsley-Kemp et al., 2019). It has been previously suggested that

the direction of extension in the Taupō rift becomes more oblique in the Okataina region (Seebeck et al., 2014), possibly influenced by the presence of a large magma reservoir (Ellis et al., 2014). Our results support these previous observations and may suggest a higher degree of rift-obliquity within the Okataina region than that proposed by Seebeck et al. (2014). However, multiple studies have also shown that dyke orientations and trajectories can be influenced by local changes to crustal stresses. Topographic loads (e.g., volcanic edifices) have been shown to modify the local stress field and cause dykes to propagate toward them (Maccaferri et al., 2011; Rivalta et al., 2015), whereas topographic depressions (e.g., calderas) promote circumferential dyke intrusions (Gaete et al., 2019). The 2019 dyke intrusion propagated toward the Tarawera volcanic edifice, perpendicular to the major OVC caldera boundary, but sub-parallel to the Puhipuhi embayment margin (Nairn, 2002, Figure 3). For comparison, the 3.4 ka Rotokawau basalt in the northwestern region of the OVC (Figure 1) erupted along a fissure that is perpendicular to both the OVC caldera and Haroharo volcanic complex, and oblique to the rift orientation (Nairn, 2002). Shortly following the Kaharoa eruption there were multiple hydrothermal eruptions SW of Tarawera. Nairn et al. (2005) propose that these were caused by the intrusion of a SW–NE oriented basaltic dyke. Similarly, the 1886 eruptive fissure extended along-axis to the SW beyond the OVC

caldera margin and into Lake Rotomahana, showing no evidence that its extent or trajectory were influenced by the OVC caldera boundary (Nairn, 1979; Nairn, 2002). This suggests that within the OVC, the load of the volcanic edifices (rather than the collapse caldera margin) are exerting a first order control on crustal stress and dyke trajectories, promoting dyke propagation toward the base of these volcanic edifices (Maccaferri et al., 2011; Rivalta et al., 2015). These are important considerations for volcanic hazard assessment and for interpreting future signals of unrest in the OVC.

Given that dyke intrusions are shown to propagate toward the volcanic edifices from outside the OVC caldera, we speculate that the basalts which have been shown to influence Tarawera eruptions are not necessarily sourced from directly beneath the volcano. A lateral migration of basaltic magma toward Tarawera may also help explain the lack of evidence for interaction with the silicic magma reservoir in the 1886 eruption (Carey et al., 2007; Carey and Houghton, 2010). In such a case, the 1886 dyke may have completely bypassed the silicic system that is presumably still present at depth (but not yet detected by geophysics) beneath Tarawera from the Kaharoa eruption in AD 1314. Alternatively, the 1886 dyke may have intersected the silicic system beneath Tarawera, but the silicic system had since cooled beyond the solidus and is now moribund. Further geophysical assessment of the magmatic plumbing system beneath the OVC is required to address these unknowns.

It is likely that the 2019 dyke intrusion may have had similarities to the early dyke intrusions that fed the 1886 Tarawera eruption. But what were the controlling factors that caused the 2019 dyke to arrest, whereas the 1886 dyke intrusion led to a deadly and violent eruption? There are numerous potential causes for the arrest of the 2019 dyke, including magma solidification within the dyke (Fialko and Rubin, 1999), pressure decrease at the source magma reservoir (Rivalta, 2010), or stress and/or structural barriers. It is also important to consider that although the earthquake activity ceased, the 2019 dyke may have continued to propagate aseismically due to the crust becoming more ductile in the region closer to the caldera boundary. If a dyke intrusion were to reach the Tarawera Volcanic complex, we suggest that the load of the Tarawera edifice would cause it to shallow (Rivalta et al., 2015) and it could then take advantage of pre-existing crustal weaknesses to propagate to the surface and erupt. This may have been the case in 1886, and if a dyke intrusion were to propagate toward, and reach, Tarawera volcano in the modern day then a similar basaltic eruption may occur. However, it's important to note that geological evidence suggests that a high flux of primitive melt is required to sustain the rhyolite volcanism observed in the TVZ (Barker et al., 2020). This means that dyke intrusions are likely to be common and thus the vast majority do not lead to an eruption. Developing a better understanding of the tipping points that cause dyke intrusions to erupt on rare occasions is an important research goal.

5.4. Implications for Monitoring and Future Activity

Our analysis of a series of earthquakes that occurred in 2019 suggests a recent dyke intrusion that propagated toward

Tarawera volcano, the site of New Zealand's largest and most destructive historical eruption (Walker et al., 1984). The OVC is monitored by GeoNet, primarily through seismometers and GNSS sensors though they are fairly sparse in the Puhupuhi embayment (Figure 2). In an active magmatic system, dyke intrusion can occur as a common process without necessarily resulting in an eruption (Acocella, 2014). However, detecting these events is critical for evaluating volcanic hazards and for monitoring ongoing surface changes. If a future dyke intrusion was identified early in its propagation, and the dyke dimensions were constrained by geodetic techniques, then the expected total mechanical energy release could be calculated using derived relationships (Bonaccorso et al., 2017; Bonaccorso and Giampiccolo, 2020). This, alongside detailed seismic analysis of the dyke-induced earthquakes, would allow for the forecast of the time and location of dyke arrest, and the associated likelihood of significant unrest and/or eruption (e.g., Aspinall et al., 2006; Constantinescu et al., 2016). We have shown that the requisite seismological analysis is possible with the current GeoNet seismic monitoring system albeit with detailed analysis long after the earthquake swarm. This process could be significantly improved using real-time detection and location of earthquakes (e.g., Chamberlain et al., 2020). However the geodetic monitoring network, particularly GNSS station density, would need to be improved in order to detect and constrain a similar future dyke intrusion. We have also shown that dyke intrusions sourced from outside the OVC caldera can propagate toward Tarawera, and we speculate that similar "external" dyke intrusions may have influenced past eruptive activity. Therefore, monitoring of Tarawera volcano should not focus solely on the region directly beneath the volcanic edifice but consider the broader surrounding area.

6. CONCLUSION

On the 12th March 2019, a swarm of 131 earthquakes occurred to the NE of Tarawera volcano, within the OVC. We use high-precision earthquake locations to demonstrate that the swarm was most likely caused by the WSW intrusion of a ~2 km long dyke, with seismicity occurring between 8 and 11 km depth. By tracking the migration of seismicity we estimate that the dyke propagated at a rate of $0.3\text{--}0.6\text{ m s}^{-1}$, a very similar propagation speed to that observed for basaltic dyke intrusions in global extensional tectonic settings. The intrusion rate, coupled with the depth of the dyke intrusion, indicate that this was most likely a basaltic dyke intrusion. Based on the dyke length and seismic moment release we estimate a total (minimum) intrusion volume of $1.1\text{--}15 \times 10^6\text{ m}^3$, and use a suite of synthetic models to show that the associated ground deformation could not have been detected by co-intrusion interferograms. The 2019 dyke intrusion propagated toward the Tarawera volcanic complex from outside the OVC, suggesting that this topographic load has a first-order control over the local crustal stress. Improvements to geodetic monitoring in the OVC could help to better identify future dyke intrusions and allow for the early assessment of the volcanic hazard they may or may not pose.

DATA AVAILABILITY STATEMENT

All seismic data used in this study are freely available from GeoNet (<https://www.geonet.org.nz/>). The earthquake catalogue is provided in QuakeML format in the Supplementary Material and as an online dataset: 10.5281/zenodo.4035171.

AUTHOR CONTRIBUTIONS

TB performed seismological analysis. FI-K supervised TB and led writing of the article. HE produced **Figure 1** and helped write the article. IH performed geodetic analysis and helped write the article. MS supervised TB and helped write the article. CW helped write the article. EM supervised TB and helped write the article. SB helped write the article.

FUNDING

TB was funded by a Victoria University of Wellington Summer Scholarship and the ECLIPSE program, which is funded by the

REFERENCES

- Acocella, V., Di Lorenzo, R., Newhall, C., and Scandone, R. (2015). An overview of recent (1988–2014) caldera unrest: knowledge and perspectives. *Rev. Geophys.* 53, 896–955. doi:10.1002/2015rg000492
- Acocella, V. (2014). Great challenges in volcanology: how does the volcano factory work? *Front. Earth Sci.* 2, 4. doi:10.3389/feart.2014.00004
- Acocella, V., Spinks, K., Cole, J. W., and Nicol, A. (2003). Oblique back arc rifting of Taupo Volcanic zone, New Zealand. *Tectonics* 22, 1045. doi:10.1029/2002tc001447
- Aspinall, W. P., Carniel, R., Jaquet, O., Woo, G., and Hincks, T. (2006). Using hidden multi-state Markov models with multi-parameter volcanic data to provide empirical evidence for alert level decision-support. *J. Volcanol. Geoth. Res.* 153, 112–124. doi:10.1016/j.jvolgeores.2005.08.010
- Bannister, S., Sherburn, S., and Bourguignon, S. (2016). Earthquake swarm activity highlights crustal faulting associated with the Waimangu–Rotomahana–Mt Tarawera geothermal field, Taupo Volcanic Zone. *J. Volcanol. Geoth. Res.* 314, 49–56. doi:10.1016/j.jvolgeores.2015.07.024
- Barker, S. J., Rowe, M. C., Wilson, C. J. N., Gamble, J. A., Rooyakkers, S. M., Wysoczanski, R. J., et al. (2020). What lies beneath? Reconstructing the primitive magmas fueling voluminous silicic volcanism using olivine-hosted melt inclusions. *Geology* 48, 504–508. doi:10.1130/g47422.1
- Barnie, T. D., Keir, D., Hamling, I., Hofmann, B., Belachew, M., Carn, S., et al. (2015). A multidisciplinary study of the final episode of the Manda Hararo dyke sequence, Ethiopia, and implications for trends in volcanism during the rifting cycle. *Geol. Soc. Lond. Spec. Pub.* 420, 149–163. doi:10.1144/sp420.6
- Belachew, M., Ebinger, C., Coté, D., Keir, D., Rowland, J., Hammond, J., et al. (2011). Comparison of dike intrusions in an incipient seafloor-spreading segment in Afar, Ethiopia: seismicity perspectives. *J. Geophys. Res.* 116, B06405. doi:10.1029/2010jb007908
- Beyreuther, M., Barsch, R., Krischer, L., Megies, T., Behr, Y., and Wassermann, J. (2010). ObsPy: a Python toolbox for seismology. *Seismol. Res. Lett.* 81, 530–533. doi:10.1785/gssrl.81.3.530
- Bibby, H. M., Caldwell, T. G., Davey, F. J., and Webb, T. H. (1995). Geophysical evidence on the structure of the Taupo Volcanic Zone and its hydrothermal circulation. *J. Volcanol. Geoth. Res.* 68, 29–58. doi:10.1016/0377-0273(95)00007-h
- Bonaccorso, A., Aoki, Y., and Rivalta, E. (2017). Dike propagation energy balance from deformation modeling and seismic release. *Geophys. Res. Lett.* 44, 5486–5494. doi:10.1002/2017gl074008
- New Zealand Ministry of Business, Innovation and Employment. FI-K, EM are fully funded, and SB, CW, IH, and MS are part supported by the ECLIPSE program. HE is part supported by the ECLIPSE program and a Victoria University of Wellington doctoral scholarship.

ACKNOWLEDGMENTS

This project analyzed and plotted the seismic data using EQcorrscan (Chamberlain et al., 2018), Obspy (Beyreuther et al., 2010), GMT (Wessel et al., 2019), and Pyrocko (Heimann et al., 2017). We thank Nico Fournier for constructive feedback on the manuscript. We also thank the constructive reviews of Yohei Yukutake and Francesca Di Luccio.

SUPPLEMENTARY MATERIAL

The Supplementary Material for this article can be found online at: <https://www.frontiersin.org/articles/10.3389/feart.2020.606992/full#supplementary-material>.

- Bonaccorso, A., and Giampiccolo, E. (2020). Balance between deformation and seismic energy release: the Dec 2018 ‘double-dike’ intrusion at Mt. Etna. *Front. Earth Sci.* 8, 463. doi:10.3389/feart.2020.583815
- Bryan, C. J., Sherburn, S., Bibby, H. M., Bannister, S. C., and Hurst, A. W. (1999). Shallow seismicity of the central Taupo Volcanic Zone, New Zealand: its distribution and nature. *N. Z. J. Geol. Geophys.* 42, 533–542. doi:10.1080/00288306.1999.9514859
- Carey, R. J., Houghton, B. F., Sable, J. E., and Wilson, C. J. N. (2007). Contrasting grain size and componentry in complex proximal deposits of the 1886 Tarawera basaltic Plinian eruption. *Bull. Volcanol.* 69, 903–926. doi:10.1007/s00445-007-0117-6
- Carey, R. J., and Houghton, B. F. (2010). “Inheritance”: an influence on the particle size of pyroclastic deposits. *Geology* 38, 347–350. doi:10.1130/g30573.1
- Cashman, K. V., and Sparks, R. S. J. (2013). How volcanoes work: a 25 year perspective. *GSA Bulletin* 125, 664–690. doi:10.1130/b30720.1
- Chambefort, I., Lewis, B., Wilson, C. J. N., Rae, A. J., Coutts, C., Bignall, G., et al. (2014). Stratigraphy and structure of the Ngatamariki geothermal system from new zircon U–Pb geochronology: implications for Taupo Volcanic Zone evolution. *J. Volcanol. Geoth. Res.* 274, 51–70. doi:10.1016/j.jvolgeores.2014.01.015
- Chamberlain, C. J., Hopp, C. J., Boese, C. M., Warren-Smith, E., Chambers, D., Chu, S. X., et al. (2018). EQcorrscan: repeating and near-repeating earthquake detection and analysis in python. *Seismol. Res. Lett.* 89, 173–181. doi:10.1785/0220170151
- Chamberlain, C. J., Townend, J., and Gerstenberger, M. C. (2020). RT-EQcorrscan: near-real-time matched-filtering for rapid development of dense earthquake catalogs. *Seismol. Res. Lett.* 1–11, 23. doi:10.1785/0220200171
- Clarke, D., Townend, J., Savage, M. K., and Bannister, S. (2009). Seismicity in the Rotorua and Kawerau geothermal systems, Taupo Volcanic Zone, New Zealand, based on improved velocity models and cross-correlation measurements. *J. Volcanol. Geoth. Res.* 180, 50–66. doi:10.1016/j.jvolgeores.2008.11.004
- Cole, J. W., Deering, C. D., Burt, R. M., Sewell, S., Shane, P. A. R., and Matthews, N. E. (2014). Okataina Volcanic Centre, Taupo Volcanic Zone, New Zealand: a review of volcanism and synchronous pluton development in an active, dominantly silicic caldera system. *Earth Sci. Rev.* 128, 1–17. doi:10.1016/j.earscirev.2013.10.008
- Cole, J. W. (1970). Petrology of the basic rocks of the Tarawera volcanic complex. *N. Z. J. Geol. Geophys.* 13, 925–936. doi:10.1080/00288306.1970.10418210

- Cole, J. W., Spinks, K. D., Deering, C. D., Nairn, I. A., and Leonard, G. S. (2010). Volcanic and structural evolution of the Okataina Volcanic Centre: dominantly silicic volcanism associated with the Taupo Rift, New Zealand. *J. Volcanol. Geoth. Res.* 190, 123–135. doi:10.1016/j.jvolgeores.2009.08.011
- Constantinescu, R., Robertson, R., Lindsay, J. M., Tonini, R., Sandri, L., Rouwet, D., et al. (2016). Application of the probabilistic model BET_UNREST during a volcanic unrest simulation exercise in Dominica, Lesser Antilles. *G-cubed* 17, 4438–4456. doi:10.1002/2016gc006485
- Darragh, M., Cole, J. W., Nairn, I. A., and Shane, P. A. R. (2006). Pyroclastic stratigraphy and eruption dynamics of the 21.9 ka Okareka and 17.6 ka Rerewhakaaitu eruption episodes from Tarawera volcano, Okataina Volcanic Centre, New Zealand. *N. Z. J. Geol. Geophys.* 49, 309–328. doi:10.1080/00288306.2006.9515170
- Dimitrova, L. L., Wallace, L. M., Haines, A. J., and Williams, C. A. (2016). High-resolution view of active tectonic deformation along the Hikurangi subduction margin and the Taupo Volcanic Zone, New Zealand. *N. Z. J. Geol. Geophys.* 59, 43–57. doi:10.1080/00288306.2015.1127823
- Eastwood, A. A., Gravley, D. M., Wilson, C. J. N., Chambefort, I., Oze, C., Cole, J. W., et al. (2013). “U-Pb dating of subsurface pyroclastic deposits (Tahorakuri Formation) at Ngatamariki and Rotokawa geothermal fields,” in Proceedings of the 35th New Zealand geothermal workshop, Rotorua, New Zealand.
- Ebinger, C. J., van Wijk, J., and Keir, D. (2013). The time scales of continental rifting: implications for global processes. *Geol. Soc. Am. Spec. Pap.* 500, 371–396. doi:10.1130/2013.2500(11)
- Efron, B., and Tibshirani, R. (1991). Statistical data analysis in the computer age. *Science* 253, 390–395. doi:10.1126/science.253.5018.390
- Efron, B., and Tibshirani, R. J. (1994). *An introduction to the bootstrap*. Boca Raton, Florida: CRC Press.
- Einarsson, P., and Brandsdóttir, B. (1980). Seismological evidence for lateral magma intrusion during the July 1978 deflation of the Krafla volcano in NE-Iceland. *J. Geophys.* 47, 160–165. doi:10.2172/890964
- Ellis, S. M., Heise, W., Kissling, W., Villamor, P., and Schreurs, G. (2014). The effect of crustal melt on rift dynamics: case study of the Taupo Volcanic Zone. *N. Z. J. Geol. Geophys.* 57, 453–458. doi:10.1080/00288306.2014.972961
- Eyles, J. H., Illsley-Kemp, F., Keir, D., Ruch, J., and Jónsson, S. (2018). Seismicity associated with the formation of a new island in the Southern Red Sea. *Front. Earth Sci.* 6, 141. doi:10.3389/feart.2018.00141
- Fialko, Y. A., and Rubin, A. M. (1999). Thermal and mechanical aspects of magma emplacement in giant dike swarms. *J. Geophys. Res.* 104, 23033–23049. doi:10.1029/1999jb900213
- Gaete, A., Kavanagh, J. L., Rivalta, E., Hazim, S. H., Walter, T. R., and Dennis, D. J. (2019). The impact of unloading stresses on post-caldera magma intrusions. *Earth Planet Sci. Lett.* 508, 109–121. doi:10.1016/j.epsl.2018.12.016
- Gamble, J. A., Smith, I. E. M., McCulloch, M. T., Graham, I. J., and Kokelaar, B. P. (1993). The geochemistry and petrogenesis of basalts from the Taupo Volcanic Zone and Kermadec island arc, SW Pacific. *J. Volcanol. Geoth. Res.* 54, 265–290. doi:10.1016/0377-0273(93)90067-2
- Gudmundsson, A. (1987). Formation and mechanics of magma reservoirs in Iceland. *Geophys. J. Int.* 91, 27–41. doi:10.1111/j.1365-246x.1987.tb05211.x
- Gudmundsson, A. (2011). Deflection of dykes into sills at discontinuities and magma-chamber formation. *Tectonophysics* 500, 50–64. doi:10.1016/j.tecto.2009.10.015
- Haines, A. J., and Wallace, L. M. (2020). New Zealand-wide geodetic strain rates using a physics-based approach. *Geophys. Res. Lett.* 47, e2019GL084606. doi:10.1029/2019gl084606
- Hamling, I. J., Ayele, A., Bennati, L., Calais, E., Ebinger, C., Keir, D., et al. (2009). Geodetic observations of the ongoing Dabbahu rifting episode: new dyke intrusions in 2006 and 2007. *Geophys. J. Int.* 178, 989–1003. doi:10.1111/j.1365-246x.2009.04163.x
- Hamling, I. J., Cevuarud, S., and Garaebiti, E. (2019). Large-scale drainage of a complex magmatic system: observations from the 2018 eruption of Ambrym volcano Vanuatu. *Geophys. Res. Lett.* 46, 4609–4617. doi:10.1029/2019gl082606
- Hamling, I. J., Hreinsdóttir, S., and Fournier, N. (2015). The ups and downs of the TVZ: geodetic observations of deformation around the Taupo Volcanic Zone, New Zealand. *J. Geophys. Res.: Sol. Earth* 120, 4667–4679. doi:10.1002/2015jb012125
- Heimann, S., Kriegerowski, M., Isken, M., Cesca, S., Daout, S., Grigoli, F., et al. (2017). *Pyrocko—an open-source seismology toolbox and library*. London: GFZ Data Services.
- Heise, W., Caldwell, T. G., Bertrand, E. A., Hill, G. J., Bennie, S. L., and Palmer, N. G. (2016). Imaging the deep source of the Rotorua and Waimangu geothermal fields, Taupo Volcanic Zone, New Zealand. *J. Volcanol. Geoth. Res.* 314, 39–48. doi:10.1016/j.jvolgeores.2015.10.017
- Heise, W., Caldwell, T. G., Bibby, H. M., and Bennie, S. L. (2010). Three-dimensional electrical resistivity image of magma beneath an active continental rift, Taupo Volcanic Zone, New Zealand. *Geophys. Res. Lett.* 37, L10301. doi:10.1029/2010gl043110
- Hogg, A. G., Higham, T. F. G., Lowe, D. J., Palmer, J. G., Reimer, P. J., and Newnham, R. M. (2003). A wiggle-match date for Polynesian settlement of New Zealand. *Antiquity* 77, 116–125. doi:10.1017/s0003598x00061408
- Holden, L., Cas, R., Fournier, N., and Ailleres, L. (2017). Modelling ground deformation patterns associated with volcanic processes at the Okataina Volcanic Centre. *J. Volcanol. Geoth. Res.* 344, 65–78. doi:10.1016/j.jvolgeores.2017.04.014
- Holden, L., Wallace, L. M., Beavan, J., Fournier, N., Cas, R., Ailleres, L., et al. (2015). Contemporary ground deformation in the Taupo rift and Okataina Volcanic Centre from 1998 to 2011, measured using GPS. *Geophys. J. Int.* 202, 2082–2105. doi:10.1093/gji/ggv243
- Hurst, T., Bannister, S., Robinson, R., and Scott, B. (2008). Characteristics of three recent earthquake sequences in the Taupo Volcanic Zone, New Zealand. *Tectonophysics* 452, 17–28. doi:10.1016/j.tecto.2008.01.017
- Illsley-Kemp, F., Savage, M. K., Wilson, C. J. N., and Bannister, S. (2019). Mapping stress and structure from subducting slab to magmatic rift: crustal seismic anisotropy of the North Island, New Zealand. *G-cubed* 20, 5038–5056. doi:10.26686/wgtn.12309776.v1
- Johnson, E. R., Kamenetsky, V. S., McPhie, J., and Wallace, P. J. (2011). Degassing of the HO-rich rhyolites of the Okataina Volcanic Center, Taupo Volcanic Zone, New Zealand. *Geology* 39, 311–314. doi:10.1130/g31543.1
- Kendall, J. M., Stuart, G. W., Ebinger, C. J., Bastow, I. D., and Keir, D. (2005). Magma-assisted rifting in Ethiopia. *Nature* 433, 146–148. doi:10.1038/nature03161
- Lamarche, G., Barnes, P. M., and Bull, J. M. (2006). Faulting and extension rate over the last 20,000 years in the offshore Whakatane Graben, New Zealand continental shelf. *Tectonics* 25, TC4005. doi:10.1029/2005tc001886
- Leonard, G. S., Cole, J. W., Nairn, I. A., and Self, S. (2002). Basalt triggering of the c. AD 1305 Kaharoa rhyolite eruption, Tarawera Volcanic Complex, New Zealand. *J. Volcanol. Geoth. Res.* 115, 461–486. doi:10.1016/s0377-0273(01)00326-2
- Lomax, A., Virieux, J., Volant, P., and Berge-Thierry, C. (2000). Probabilistic earthquake location in 3D and layered models. *Mod. Approaches Geophys.* 18, 101–134. doi:10.1007/978-94-015-9536-0_5
- Maccaferri, F., Bonafede, M., and Rivalta, E. (2011). A quantitative study of the mechanisms governing dike propagation, dike arrest and sill formation. *J. Volcanol. Geoth. Res.* 208, 39–50. doi:10.1016/j.jvolgeores.2011.09.001
- Mantiloni, L., Nespoli, M., Belardinelli, M. E., and Bonafede, M. (2020). Deformation and stress in hydrothermal regions: the case of a disk-shaped inclusion in a half-space. *J. Volcanol. Geoth. Res.* 403, 107011. doi:10.1016/j.jvolgeores.2020.107011
- Martí, J., Pínel, V., López, C., Geyer, A., Abella, R., Tárraga, M., et al. (2013). Causes and mechanisms of the 2011–2012 El Hierro (Canary Islands) submarine eruption. *J. Geophys. Res.: Sol. Earth* 118, 823–839. doi:10.1002/jgrb.50087
- Moran, S. C., Newhall, C., and Roman, D. C. (2011). Failed magmatic eruptions: late-stage cessation of magma ascent. *Bull. Volcanol.* 73, 115–122. doi:10.1007/s00445-010-0444-x
- Nairn, I. A. (2002). *Geology of the Okataina Volcanic Center, scale 1:50,000*, 25. New Zealand: Institute of Geological and Nuclear Sciences Geological Map, Lower Hutt.
- Nairn, I. A., and Cole, J. W. (1981). Basalt dikes in the 1886 Tarawera rift. *N. Z. J. Geol. Geophys.* 24, 585–592. doi:10.1080/00288306.1981.10421534
- Nairn, I. A., Hedenquist, J. W., Villamor, P., Berryman, K. R., and Shane, P. A. (2005). The AD1315 Tarawera and Waiotapu eruptions, New Zealand: contemporaneous rhyolite and hydrothermal eruptions driven by an arrested basalt dike system?. *Bull. Volcanol.* 67, 186–193. doi:10.1007/s00445-004-0373-7

- Nairn, I. A. (1979). Rotomahana—Waimangu eruption, 1886: base surge and basalt magma. *N. Z. J. Geol. Geophys.* 22, 363–378. doi:10.1080/00288306.1979.10424105
- Nairn, I. A., Shane, P. R., Cole, J. W., Leonard, G. J., Self, S., and Pearson, N. (2004). Rhyolite magma processes of the AD 1315 Kaharoa eruption episode, Tarawera volcano, New Zealand. *J. Volcanol. Geoth. Res.* 131, 265–294. doi:10.1016/s0377-0273(03)00381-0
- Nairn, I. A. (1992). The Te Rere and Okareka eruptive episodes—Okataina Volcanic Centre, Taupo Volcanic Zone, New Zealand. *N. Z. J. Geol. Geophys.* 35, 93–108. doi:10.1080/00288306.1992.9514503
- Nicholls, I. A., Oba, T., and Conrad, W. K. (1992). The nature of primary rhyolitic magmas involved in crustal evolution: evidence from an experimental study of cummingtonite-bearing rhyolites, Taupo Volcanic Zone, New Zealand. *Geochem. Cosmochim. Acta* 56, 955–962. doi:10.1016/0016-7037(92)90039-1
- Pugh, D. J., and White, R. S. (2018). MTfit: a Bayesian approach to seismic moment tensor inversion. *Seismol. Res. Lett.* 89, 1507–1513. doi:10.1785/0220170273
- Ristau, J., Harte, D., and Salichon, J. (2016). A revised local magnitude (M_L) scale for New Zealand earthquakes. *Bull. Seismol. Soc. Am.* 106, 398–407. doi:10.1785/0120150293
- Rivalta, E. (2010). Evidence that coupling to magma chambers controls the volume history and velocity of laterally propagating intrusions. *J. Geophys. Res.* 115, B07203. doi:10.1029/2009jb006922
- Rivalta, E., Taisne, B., Bungler, A. P., and Katz, R. F. (2015). A review of mechanical models of dike propagation: schools of thought, results and future directions. *Tectonophysics* 638, 1–42. doi:10.1016/j.tecto.2014.10.003
- Roland, E., and McGuire, J. J. (2009). Earthquake swarms on transform faults. *Geophys. J. Int.* 178, 1677–1690. doi:10.1111/j.1365-246x.2009.04214.x
- Rowland, J. V., and Sibson, R. H. (2001). Extensional fault kinematics within the Taupo Volcanic Zone, New Zealand: soft-linked segmentation of a continental rift system. *N. Z. J. Geol. Geophys.* 44, 271–283. doi:10.1080/00288306.2001.9514938
- Rowland, J. V., Wilson, C. J. N., and Gravley, D. M. (2010). Spatial and temporal variations in magma-assisted rifting, Taupo Volcanic Zone, New Zealand. *J. Volcanol. Geoth. Res.* 190, 89–108. doi:10.1016/j.jvolgeores.2009.05.004
- Sable, J. E., Houghton, B. F., Wilson, C. J. N., and Carey, R. J. (2006). Complex proximal sedimentation from Plinian plumes: the example of Tarawera 1886. *Bull. Volcanol.* 69, 89–103. doi:10.1007/s00445-006-0057-6
- Sandri, L., Acocella, V., and Newhall, C. (2017). Searching for patterns in caldera unrest. *G-cubed* 18, 2748–2768. doi:10.1002/2017gc006870
- Seebeck, H., Nicol, A., Villamor, P., Ristau, J., and Pettinga, J. (2014). Structure and kinematics of the Taupo rift, New Zealand. *Tectonics* 33, 1178–1199. doi:10.1002/2014tc003569
- Shane, P., Martin, S. B., Smith, V. C., Beggs, K. F., Darragh, M. B., Cole, J. W., et al. (2007). Multiple rhyolite magmas and basalt injection in the 17.7 ka Rerewhakaaitu eruption episode from Tarawera volcanic complex, New Zealand. *J. Volcanol. Geoth. Res.* 164, 1–26. doi:10.1016/j.jvolgeores.2007.04.003
- Shane, P., Nairn, I. A., Smith, V. C., Darragh, M., Beggs, K., and Cole, J. W. (2008). Silicic recharge of multiple rhyolite magmas by basaltic intrusion during the 22.6 ka Okareka Eruption Episode, New Zealand. *Lithos* 103, 527–549. doi:10.1016/j.lithos.2007.11.002
- Sherburn, S., and Nairn, I. A. (2004). Modelling geophysical precursors to the prehistoric c. AD1305 Kaharoa rhyolite eruption of Tarawera volcano, New Zealand. *Nat. Hazards* 32, 37–58. doi:10.1023/b:nhaz.0000026791.16566.96
- Sigmundsson, F., Hooper, A., Hreinsdóttir, S., Vogfjörð, K. S., Ófeigsson, B. G., Heimisson, E. R., et al. (2015). Segmented lateral dyke growth in a rifting event at Bárðarbunga volcanic system, Iceland. *Nature* 517, 191–195. doi:10.1038/nature14111
- Smith, E. G. C., Williams, T. D., and Darby, D. J. (2007). Principal component analysis and modeling of the subsidence of the shoreline of Lake Taupo, New Zealand, 1983–1999: evidence for dewatering of a magmatic intrusion?. *J. Geophys. Res.* 112, B08406. doi:10.1029/2006jb004652
- Sparks, R. S., Biggs, J., and Neuberg, J. W. (2012). Monitoring volcanoes. *Science* 335, 1310–1311. doi:10.1126/science.1219485
- Tentime, T., Biggs, J., Lewi, E., and Ayele, A. (2020). Evidence for active rhyolitic dike intrusion in the Northern Main Ethiopian Rift from the 2015 Fentale seismic swarm. *G-cubed* 21, e2019GC008550. doi:10.1029/2019gc008550
- Townend, J., Sherburn, S., Arnold, R., Boese, C., and Woods, L. (2012). Three-dimensional variations in present-day tectonic stress along the Australia–Pacific plate boundary in New Zealand. *Earth Planet. Sci. Lett.* 353–354, 47–59. doi:10.1016/j.epsl.2012.08.003
- Trugman, D. T., and Shearer, P. M. (2017). GrowClust: a hierarchical clustering algorithm for relative earthquake relocation, with application to the Spanish Springs and Sheldon, Nevada, earthquake sequences. *Seismol. Res. Lett.* 88, 379–391. doi:10.1785/0220160188
- Villamor, P., Berryman, K. R., Nairn, I. A., Wilson, K., Litchfield, N., and Ries, W. (2011). Associations between volcanic eruptions from Okataina volcanic center and surface rupture of nearby active faults, Taupo rift, New Zealand: insights into the nature of volcano-tectonic interactions. *Bull. Geol. Soc. Am.* 123, 1383–1405. doi:10.1130/b30184.1
- Wadge, G., Biggs, J., Lloyd, R., and Kendall, J.-M. (2016). Historical volcanism and the state of stress in the East African Rift system. *Front. Earth Sci.* 4, 86. doi:10.3389/feart.2016.00086
- Waight, T. E., Troll, V. R., Gamble, J. A., Price, R. C., and Chadwick, J. P. (2017). Hf isotope evidence for variable slab input and crustal addition in basalts and andesites of the Taupo Volcanic Zone, New Zealand. *Lithos* 284, 222–236. doi:10.1016/j.lithos.2017.04.009
- Waite, G. P., and Smith, R. B. (2002). Seismic evidence for fluid migration accompanying subsidence of the Yellowstone caldera. *J. Geophys. Res.: Sol. Earth* 107, 2177. doi:10.1029/2001JB000586
- Walker, G. P., Self, S., and Wilson, L. (1984). Tarawera 1886, New Zealand—a basaltic plinian fissure eruption. *J. Volcanol. Geoth. Res.* 21, 61–78. doi:10.1016/0377-0273(84)90016-7
- Wallace, L. M., Beavan, J., McCaffrey, R., and Darby, D. (2004). Subduction zone coupling and tectonic block rotations in the North Island, New Zealand. *J. Geophys. Res.: Sol. Earth* 109, B12406. doi:10.1029/2004jb003241
- Wessel, P., Luis, J. F., Uieda, L., Scharroo, R., Wobbe, F., Smith, W. H. F., et al. (2019). The generic mapping tools version 6. *G-cubed* 20, 5556–5564. doi:10.5194/egusphere-egu2020-2245
- Wilson, C. J. N., Houghton, B. F., McWilliams, M. O., Lanphere, M. A., Weaver, S. D., and Briggs, R. M. (1995). Volcanic and structural evolution of Taupo Volcanic Zone, New Zealand: a review. *J. Volcanol. Geoth. Res.* 68, 1–28. doi:10.1016/0377-0273(95)00006-g
- Wilson, C. J. N. (2017). Volcanoes: characteristics, tipping points, and those pesky unknown unknowns. *Elements* 13, 41–46. doi:10.2113/gselements.13.1.41

Conflict of Interest: The authors declare that the research was conducted in the absence of any commercial or financial relationships that could be construed as a potential conflict of interest.

Copyright © 2021 Benson, Illsley-Kemp, Elms, Hamling, Savage, Wilson, Mestel and Barker. This is an open-access article distributed under the terms of the Creative Commons Attribution License (CC BY). The use, distribution or reproduction in other forums is permitted, provided the original author(s) and the copyright owner(s) are credited and that the original publication in this journal is cited, in accordance with accepted academic practice. No use, distribution or reproduction is permitted which does not comply with these terms.